Structure, Dynamics, and Interaction of the Stationary Phase and Xenon Atoms in the Zorbax SB-C18 HPLC Column Material Studied by Solid State NMR and ^{129}Xe NMR

Yong Ba* and Danny Chagolla

Department of Chemistry and Biochemistry, California State University, Los Angeles, 5151 State University Drive, Los Angeles, California 90032

Received: December 19, 2001; In Final Form: March 19, 2002

This research applied the techniques of CP MAS ^{29}Si and ^{13}C, MAS high power decoupling ^{13}C, and MAS ^{1}H solid-state NMR, variable-temperature dependent ^{1}H NMR, ^{129}Xe NMR, low temperature ^{1}H diffusion, and two-dimensional exchange ^{129}Xe NMR to study the structure, dynamics, and interaction of the stationary phase and the xenon atoms in the Zorbax SB-C18 HPLC column material. The solid-state NMR experimental results showed the single binding type of alkylsilane groups, $-Si(CH_2-CH-(CH_3)_2)_2(CH_2)_{17}CH_3$, and the mobile alkyl chains on the silica surface at room temperature. The VT ^{1}H NMR and ^{1}H spin diffusion experiments suggested that at low temperatures a large portion of the alkyl chain molecules became immobile in the area where the density of the alkyl chains could be higher, while the rest of the alkyl chains remained somehow mobile in the areas with possibly lower density. The results of the VT ^{129}Xe NMR experiments showed the solvation of the xenon atoms in the stationary phase, the spatial occupation of the xenon atoms in the void spaces of the column material, and the diffusion of the xenon atoms in the column material. The two-dimensional exchange ^{129}Xe NMR results at low temperatures displayed the slow xenon diffusion between the pores and the voids between the particles. The two-dimensional exchange ^{129}Xe NMR spectra also indicate that the amorphous areas of the alkyl chains in the stationary phase experienced slow motions even at a temperature of −140 °C. This research illustrated that solid-state NMR of the stationary phase and ^{129}Xe NMR of the mobile phase give complementary information concerning the structure, dynamics, and interaction of column materials.

I. Introduction

Chromatography is a powerful method that finds application in the separation of mixtures.[1−3] Bonded stationary phases of chromatographic column materials are made of siloxane coatings on porous silica or silica-based substances, which are formed as uniform, porous, and mechanically sturdy particles. The long-chain hydrocarbon groups are generally aligned parallel to each other and perpendicular to the particle surface, providing a brush-like structure. The properties of retaining molecules on the surfaces of the stationary phases are critical for molecular separations. Chromatographic characterizations provide information about the relationship between the stationary phase variables and the mobile phase properties, but detailed molecular interactions and dynamics could not be studied. The goal of this research is to study the retention mechanisms of chromatographic column materials from the point of view of molecular structure, dynamics, and interaction, by means of solid-state NMR and mobile phase xenon NMR techniques.

Solid state NMR has been widely used to study material structures, especially for studying short-range order of materials and molecular dynamics. Recently, ^{1}H, ^{13}C, and ^{29}Si solid-state NMR experiments were used to study the chain structure and mobility of the stationary phases of liquid chromatographic column materials.[4−8] It was shown that high-speed magic angle spinning (MAS) ^{1}H NMR spectra could give well-resolved spectral resolution for the stationary phase molecules because of the high mobility of the alkyl chains on the silica surfaces. The chain order and mobility could also be detected by the cross polarization (CP) MAS ^{13}C NMR spectra, where the trans conformation and the dynamically averaged trans and gauche conformations can be distinguished by the different ^{13}C chemical shifts. CP MAS ^{29}Si NMR was shown to be useful to detect the structurally different siloxane/alkylsilane species formed on the silica surfaces. To study the retention mechanisms of column materials, besides the stationary phase, it is also necessary to study the mobile phase properties, such as the molecular diffusion and interaction between the mobile-phase molecules and the stationary-phase molecules. In searching for a probe to determine these properties, we think xenon is an ideal candidate. Xenon is sensitive for local environments and interactions because of its large polarizability, which results in a wide ^{129}Xe NMR chemical shift range. Together with xenon's relative inertness, the sensitivity of its NMR parameters to local environments enables a variety of different interactions, surrounding structures, and motions to be probed.[9] A wide range of applications of xenon NMR have been carried out for the study of microporous materials, such as molecular sieves and zeolitic-inclusion materials,[10−19] and for the study of structural heterogeneous polymers.[20−24] In addition, xenon's exchange and diffusion parameters[25] can provide important information about the spatial pores, channels and micro transportation processes in a porous material.

In this paper, we will first show the structural and dynamic information of a commercial Zorbax SB−C18 column material obtained by ^{13}C, ^{29}Si, and ^{1}H solid-state NMR techniques. Then, we will discuss the surface morphological changes with different

* To whom correspondence should be addressed. Phone: (323) 343-2360. Fax: (323) 343-6490. E-mail: yba@calstatela.edu.

10.1021/jp014600b CCC: $22.00
Published on Web 04/27/2002

temperatures, studied by variable temperature (VT) dependent ^{1}H NMR experiments. Finally, we will demonstrate the applicability of ^{129}Xe NMR to probe the chain structure and dynamics of the stationary phase and the porosity of the column material by VT dependent and two-dimensional (2D) exchange ^{129}Xe NMR experiments.

II. Experimental Section

The Zorbax SB-C18 HPLC column material was commercially purchased from Agilent Technologies. This material was produced from porous silica reacted with chlorodiisobutyoctadecylsilane. The formula of this material was given to be $(SiO_2)_x[Si(CH_2-CH-(CH_3)_2)_2(CH_2)_{17}CH_3]_y$. The diameter of the silica particle size is 5 μm, the diameter of the pore size is 80 Å, the surface area is 180 m^2/g, and the surface coverage is 2.0 μ mol/m^2. The xenon gas (purity 99.995%) was purchased from AGA Specialty Gas. Heavy walled 10 mm NMR tubes with wall thickness of 1.45 mm, purchased from WILMAD, were used for the xenon NMR experiments. The sample of the column material mixed with xenon was prepared on a vacuum line by removing air and then adding xenon gas at a controlled pressure into the NMR sample tube. The NMR tube was then frozen and sealed in liquid nitrogen. The pressure of xenon gas inside the NMR tube was determined to be 5.9 atm at room temperature (22 °C).

The NMR experiments were carried out with a Bruker DRX 400 NMR spectrometer. A Bruker 7 mm CP MAS NMR probe was used for the ^{1}H MAS, ^{13}C CP MAS, ^{29}Si CP MAS, and proton high power decoupling ^{13}C MAS NMR experiments. The MAS frequencies of 4.2, 3.3, and 1.9 kHz were used for the ^{1}H, ^{29}Si, and ^{13}C NMR experiments, respectively. ^{1}H 90° pulse lengths of 7.0 μs and recycling delays of 5 s were used for the first three NMR experiments, and a recycling delay of 20 s was used for the last experiment. A contact time of 1 ms was used for the ^{13}C CP MAS experiment, and 3 ms was used for the ^{29}Si CP MAS experiment. TMS was used as a reference for the ^{1}H, ^{13}C and ^{29}Si chemical shifts. A Bruker X−H 10 mm high-resolution NMR probe was used for the ^{129}Xe NMR experiments. A 90° pulse length of 8 μs with a recycling delay of 6 s was used for these experiments. The chemical shift at 0 atm, which was obtained from the extrapolation of the plot of ^{129}Xe chemical shifts versus the pressures of the xenon gas, was used as reference for ^{129}Xe chemical shift. The pulse sequence of the 2D exchange NMR spectroscopy (EXSY) described in refs 26−28 was employed for the ^{129}Xe EXSY experiments. The temperatures for the experiments were carefully manipulated. After a temperature was reached, the ^{129}Xe NMR spectrum was acquired every 6 min to make sure that the sample had reached equilibrium before a final spectrum was acquired. The Bruker X−H 10 mm high-resolution NMR probe was also used for the VT static ^{1}H NMR experiments, where the column material filled with xenon gas was used. A ^{1}H 90° pulse length of 10 μs, with a recycling delay of 10 s was used for this experiment. In the proton spin diffusion experiment,[29] the T_2 selective method was used to obtain the magnetization with longer T_2 time or narrower NMR peak. The selected magnetization along the z axis and $-z$ axis were alternated during the experiment in order to cancel the magnetization grown from the relaxation process during the spin diffusion time.

III. Results and Discussion

Figure 1 shows the CP MAS ^{29}Si NMR spectrum of the SB−C18 column material. Three peaks at −110.8, −101.4 and +11.6 ppm were clearly detected, and one lower left shoulder around

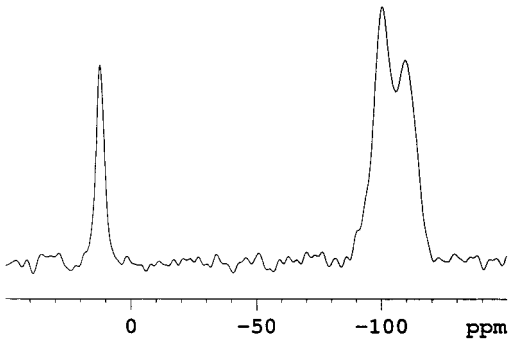

Figure 1. CP MAS ^{29}Si NMR spectrum of the Zorbax SB−C18 column material. The peaks at −110.8 and −101.4 ppm arise from the Q^4 and Q^3 sites, respectively, and the lower shoulder at −92 ppm is from the Q^2 site. The peak at 11.6 pm is due to the ^{29}Si signal from the alkylsilane group, $-Si(CH_2-CH-(CH_3)_2)_2(CH2)_{17}CH_3$.

−92.0 ppm can be recognized. Engelhardt et al.,[30] in a study of "^{29}Si NMR of inorganic solids", summarized that Q^4 silicon has a chemical shift range from −107 to −120 ppm, Q^3 silicon (single silanol silicon) has a chemical shift range from −91 to −103 ppm, Q^2 (geminal silanol silicon) has a chemical shift range from −74 to −93 ppm, and Q^1 and Q^0 have lower chemical shifts. We, therefore, assign the peaks at −110.8 and −101.4 ppm to the Q^4 and Q^3 silicon sites in the SB−C18 column material, respectively, and the shoulder at ∼ −92.0 ppm to be the Q^2 silicon. Pursch et al.[8] in a ^{29}Si NMR study of a C18 ($-Si(CH_3)_2(CH2)_{17}CH_3$) phase column material showed that the ^{29}Si chemical shift in the alkylsilane groups is around 12 ppm. Therefore, the peak at 11.6 pm in Figure 1 arise from the ^{29}Si signal from the alkylsilane groups, $-Si(CH_2-CH-(CH_3)_2)_2(CH2)_{17}CH_3$, anchored on the silica surface. Pursch et al. also showed that ^{29}Si chemical shifts of silanol groups and alkylsilanes cross-linked through Si−O−Si bridges are from 0 to −80 ppm. No such signals in this range were observed from the SB−C18 column material, indicating that no cross-linking between the alkylsilane groups was produced during the synthesis of the column materials, and only one type of alkylsilanes was coated on the silica surface.

Figure 2 parts a and b shows the CP MAS ^{13}C NMR spectrum and the proton high power decoupling MAS ^{13}C NMR spectrum of the SB−C18 column material. The major peaks in both spectra are at 30.4 ppm representing the alkyl chains $-(CH_2)_n-CH_3$ for $n = 4-15$, because the substituent effect of the end groups on alkyl chains can only be observed within four bonds.[6] This chemical shift arises from the average of the chemical shifts of the trans and gauche conformations of the alkyl chains,[31,32] showing that the alkyl chains on the silica surface are quite mobile at room temperature, and the alkyl chains experienced fast trans and gauche conformational exchange on the ^{13}C NMR time-scale. A small peak at 32.5 ppm is close to the chemical shift value of the alkyl chains with trans conformation, which, at first glance, seems to show the rigid trans alkyl chains on the silica surface. However, when comparing the relative intensities of this peak to the major peak at 30.4 ppm, we found that the intensity is bigger in spectrum b than that in spectrum a. This implies that the small peak at 32.5 ppm represents a carbon site that is more mobile than those of the major chains because of the motional average for the cross-polarization process. After comparison with the assignments of the ^{13}C chemical shifts of a C18 column material studied by Pursch et al.,[8] we assign this peak to the C16 in the alkyl chains. By similar comparison, we assign the peak at 22.9 ppm to the C17 in the alkyl chains. The intensity difference for this peak between

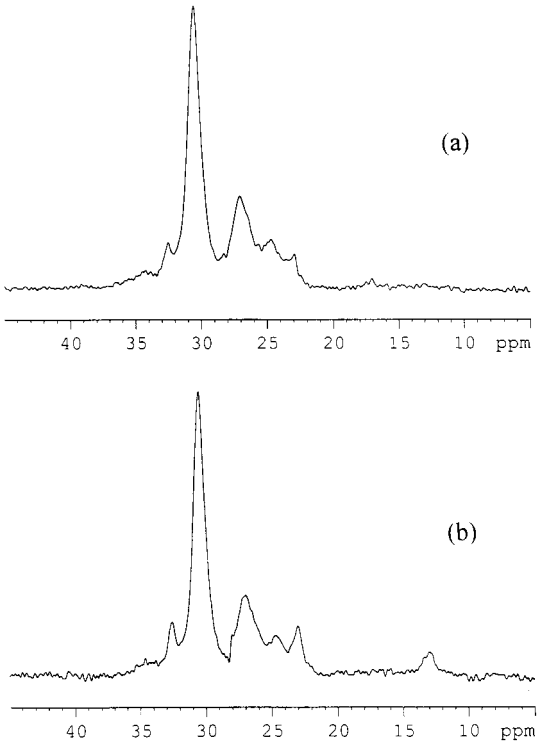

Figure 2. Spectra a and b show the CP MAS ^{13}C NMR spectrum and the proton high power decoupling MAS ^{13}C NMR spectrum of the SB−C18 column material. The major peak in both spectra at 30.4 ppm is due to the alkyl chain carbons, $-(CH_2)_nCH_3$, for $n = 4-15$. The small peaks at 32.5, 22.9, and 13.0 ppm represent the carbons for $n = 16$ and 17 and the terminal methyl group, respectively. The small peaks at 34.3, 24.7, and 17.0 ppm (only appears in a) represent the carbons for $n = 3$, 2, and 1, respectively. The second major peak at 26.9 ppm in both spectra a and b could represent the $-CH_3$ carbon in the side group, $Si-(CH_2-CH-(CH_3)_2)_2$. The signal at 28.5 ppm in (a) might come from the −CH− group in the side chain, and the chemical shift of the C1 carbon in the side chain might be in the region at 17 ppm.

spectra a and b is even bigger than that for the peak at 32.5 ppm, which indicates that C17 is even more mobile than C16 in the chain. It is noticeable that the peak at 13.0 ppm is only obtained in spectrum b but barely observed in spectrum a, which indicates that this carbon is almost liquidlike. Thus, this peak should represent the methyl groups (C18) at the terminals of the alkyl chains. This assignment is also in agreement with that in Pursch's paper. According to the paper of Pursch et al., the chemical shift of C3 is close to that of C16, C2, to C17 and C1 to C18 on the low field sides. Therefore, we assign the peak at 34.3 ppm to C3, the peak at 24.7 ppm to C2, and the peak at 17.0 ppm to C1. The peak at 17.0 ppm looks quite weak and only appears in spectrum a. This could be due to the long relaxation time of C1, because of the rigidity of this carbon, which also results in a bigger chemical shift anisotropy. The second major peak at 26.9 ppm in both spectra a and b does not exist for the C18 column material made of the alkylsilanes, $-Si(CH_3)_2(CH_2)_{17}CH_3$.[8] Therefore, this peak must come from the side group, $Si-CH_2-CH-(CH_3)_2$ in this SB−C18 column material. We tentatively assign this peak to $-CH_3$ in the side group, because of its relative intensity compared to the major peak. When we compare spectra a and b carefully, we can see that there is another peak at about 28.5 ppm shown in spectrum a. This signal might come from the −CH− group in the side chain. The reason this signal is not obvious in spectrum b could be due to the long relaxation time resulting from the rigidity of this carbon. For the same reason as for the C1 carbon in the main chains, the chemical shift anisotropy of the C1 carbon in the side chain could be very big, and its signal might also be in the 17 ppm region.

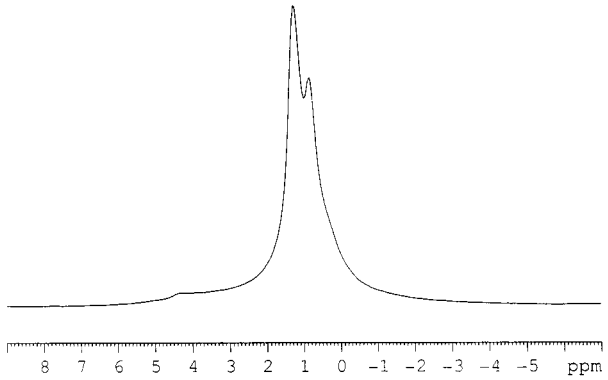

Figure 3. ^1H MAS NMR spectrum of the SB−C18 column material. The peaks at 0.8 and at 1.2 ppm represent the $-CH_3$ group and the $-CH_2-$ group in the alkyl chains, respectively. A small peak at 4.3 ppm might be due to the protons in the single silanols hydrogen-bonded to water molecules.

Figure 3 shows the ^1H MAS NMR spectrum of the SB−C18 column material, where only the central bands are shown (but not the MAS sidebands). Three peaks are resolved in this spectrum. Two large peaks are at 0.8 and 1.2 ppm and one small peak is at 4.3 ppm. The chemical shift for the protons of $R-CH_3$ is known to be 0.9 ppm, and that of the protons of $R-CH_2-R'$ to be 1.3 ppm, where R and R′ represent alkyl groups. Therefore, we attribute the peak at 0.8 ppm to $-CH_3$ groups and the peak at 1.2 ppm to $-CH_2-$ groups in the C-18 chains, after considering the inherent chemical shift error caused by the broad solid-state NMR line widths. CRAMPS ^1H NMR on silica gels studies by Maciel et al.[33−35] showed that isolated SiOH has a proton chemical shift at 1.7 ppm, and dipolar coupled SiOH protons on a silica surface show a broad line with a chemical shift range from 1 to 8 ppm. The ^{29}Si NMR spectrum in Figure 1 shows the Q^3 and Q^2 silicon peaks, verifying the existence of the silanol groups in the SB−C18 column material. However, these silanol proton signals cannot be resolved from the MAS spectrum. We believe the broad line shape of the silanol groups on silica surface is overwhelmed by the proton signal of the alkylsilane groups in the spectrum. A proton NMR study on amorphous silicas by Dorémieur-Morin et al.[36] demonstrated that the hydrogen atoms of single silanol hydrogen-bonded to water molecules have a MAS peak between 3.9 and 4.7 ppm because of the rapid exchange of protons between the water and the silanol. Thus, the small peak at 4.3 ppm could be attributed to the single silanol groups hydrogen-bonded to water molecules. The good resolution of the MAS proton NMR spectrum of the alkyl chains in Figure 1 indicates that they are quite mobile in the stationary phase at room temperature, resulting in the average of the proton dipolar interactions, which is in agreement with the above-discussed ^{13}C NMR spectra.

The alkyl chain mobility in the stationary phase at different temperatures was monitored by static ^1H NMR spectra. These spectra are shown in Figure 4, where the sampling temperatures are labeled with their corresponding spectra. The sample of the SB−C18 column material mixed with the xenon gas was used to obtain these spectra. At room temperature, the line width of the ^1H spectrum is quite narrow (about 4 kHz) compared with that of a bulk organic solid (typically 50−100 kHz), and even the two chemical shifts from $-CH_3$ and $-CH_2-$ groups can be slightly resolved in the static condition. This shows that the alkyl chains experienced both rotational and translational motions with frequencies bigger than tens of thousands kHz,

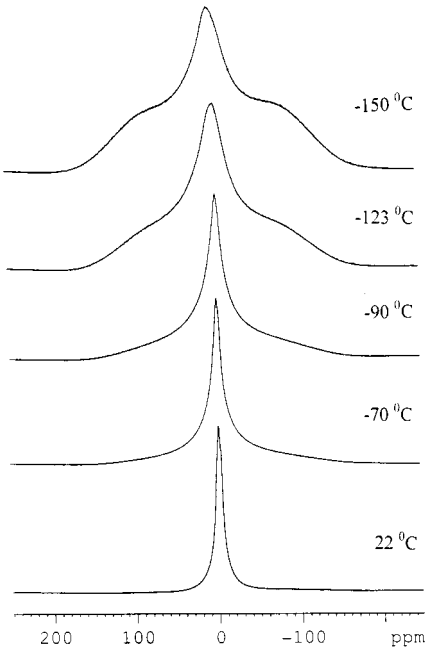

Figure 4. VT dependent static ^{1}H NMR spectra of the SB−C18 column material with the xenon gas mixed inside. At room temperature, the narrower line shape shows the alkyl chains with high mobility in the stationary phase. The broader components in the spectra at lower temperatures are from the immobile area of the stationary phase on the silica surface, and the narrower components arise from the mobile area.

which somehow averages out both the intra- and interchain proton dipolar interactions. With decreasing temperature, a broader component gradually emerged in the spectra, a feature that became obvious starting at −70 °C. The relative intensity and line width of this broader component continued to increase when the temperature was further decreased. At −150 °C, the line width of the broad component reached ∼100 kHz, and that of the narrow component is about 16 kHz. The ratio of the broad component to the narrow component is about 5:1 at this temperature. A similar ^{1}H NMR spectral pattern was observed for high-density polyethylene and polyoxymethylene,[37,38] where the broad line shapes arise from the rigid crystalline domains, and the narrow line shapes arise from the amorphous domains. We think that, similar to the high-density polymers, the broad line shapes at low temperatures in Figure 4 could represent the local surface area of the immobile alkyl chains, and the narrow line shapes could arise from the local surface area of the mobile alkyl chains for the SB−C18 column material. To see if the narrower and broader peaks arose from different areas on the silica surface or were caused by different dynamics along the chains, a proton spin diffusion experiment[29] was carried out at −120 °C. The magnetization component of the narrower peak was selected by allowing the transverse magnetization to decay for 16 μs after a 90° pulse and was then brought back to the z axis by another 90° pulse. After a spin diffusion time was given, another 90° pulse was applied to acquire the proton NMR spectrum. The experimental spectra with 5 ms and 2 s mixing times are shown in Figure 5 where the spin diffusion times are labeled with the corresponding spectra. It shows that even when a 2 s spin diffusion time was used no broader peak was generated. This means that the protons represented by the narrower peak are spatially separated (by at least several angstroms) from the protons represented by the broad peak. The spin diffusion experiment excludes the possibility that the broader component and the narrower component are caused by

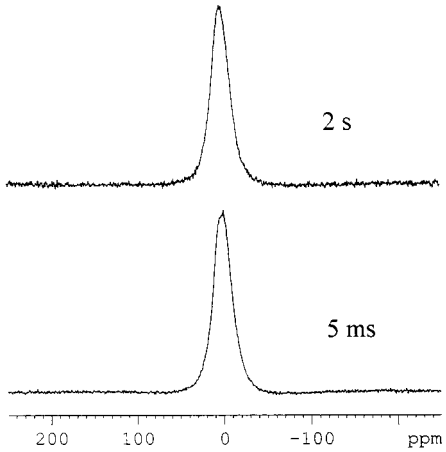

Figure 5. Proton spin diffusion experiment at −120 °C. The magnetization component of the narrower peak in the spectrum of Figure 4 was selected for monitoring the spin diffusion. The experimental spectra with 5 ms and 2 s mixing times indicate that the protons represented by the narrower peak are spatially separated from the protons represented by the broad component.

different dynamics along the alkyl chains. The immobile chains should be formed on the area where the density of the alkyl chains is higher, by possibly a folding and closely packing of the alkyl chains, and the mobile chains should come from the area where the density of the alkyl chains is lower. It is, therefore, concluded that the alkyl chains on the silica surface are distributed from higher density to lower density, a feature reflected by the gradual increase of the broader component of the proton spectra with decreasing temperatures.

In the following, we will discuss the ^{129}Xe NMR spectra of xenon gas compressed in the SB−C18 column material. Figure 6 shows the VT dependent ^{129}Xe NMR spectra, which are labeled with their corresponding experimental temperatures. The spectrum at 22 °C consists of a sharp peak at 3.0 ppm and a broad peak at 54.5 ppm. The sharp peak is from the gas phase xenon showing the freely tumbling xenon atoms inside the silica pores and the spaces between the silica particles. The broad signal is from the solvated xenon in the stationary phase showing the interaction of xenon atoms with the alkyl chains in the stationary phase. The ^{129}Xe chemical shift for the xenon solvated in the stationary phase increased when the temperature was lowered. The line width also became larger with decreasing temperature, indicating enhanced anisotropic interactions between xenon atoms and the stationary phase molecules. At −55 °C, it appears that the two line shapes overlap. A broader line width indicates larger anisotropic interactions between xenon and its local environment. Thus, the broader component could arise from xenon solvated in the less mobile area of the stationary phase, and the narrower one on the left top region could come from xenon solvated in the more mobile area of the stationary phase. Figure 6 also shows that, from +22 °C to −55 °C, the relative signal intensity of the stationary phase increased compared with the gas-phase signal indicating that xenon's solvation in the stationary phase increased with the gradual decreasing of the temperature.

At −70 °C, a sharp peak at 227.4 ppm began to form. The Xe NMR study shows that liquid xenon has a chemical shift range from 150 to 240 ppm.[9] After also considering the sharpness of this peak, we attribute the peak to the liquid xenon condensed in the pores and the spaces between the silica particles. Xenon has a normal boiling point of −108 °C. However, the boiling point increases when the pressure is higher. In a study of xenon NMR of mesoporous silicas by Pietrass et

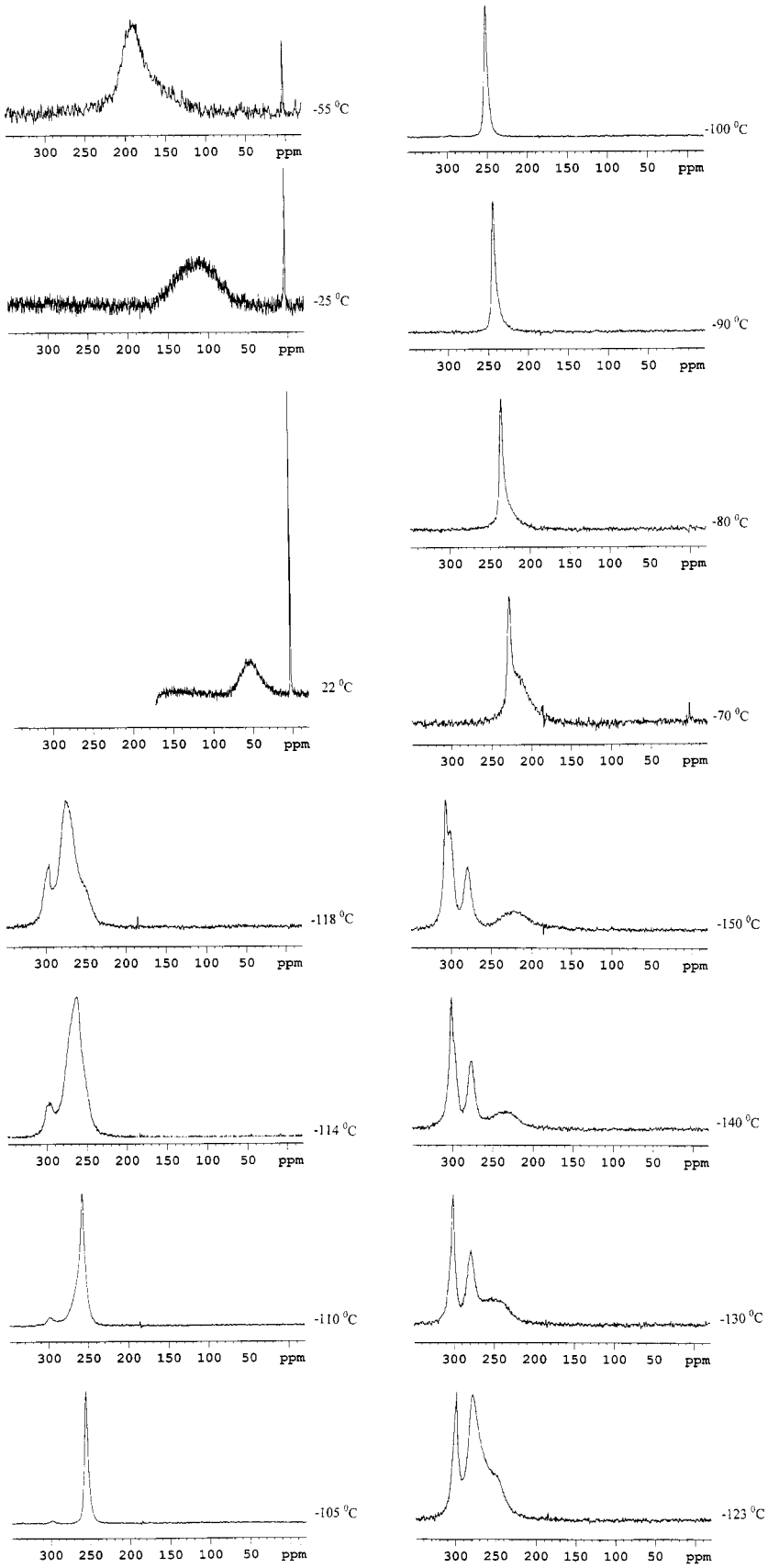

Figure 6. VT ^{129}Xe NMR spectra of xenon in the SB−C18 column material. The experimental temperatures are labeled with their corresponding spectra. At 22 °C, the sharp peak at 3.0 ppm shows the gas-phase xenon inside the silica pores and the spaces between the silica particles, and the broad peak at 54.5 ppm shows the xenon solvated in the stationary phase. At −70 °C, the sharp peak at 227.4 ppm arises from the liquid xenon inside the silica pores and the spaces between the silica particles, and the broader peak at 211.9 ppm is due to the solvated xenon in the stationary phase. At −150 °C, the peaks at 302.9, 297.4, and 276.5 ppm arise from the solid xenon possibly outside the column material, in the spaces between the silica particles, and in the pores of the silica particles, respectively, and the peak at 219.7 ppm is from the xenon trapped in the stationary phase of the column material.

al.,[18] the boiling point of xenon at 4.1 atm was predicted to be −73 °C. Thus, the pressure of xenon at −70 °C should be slightly higher than 4.1 atm. The pressure of xenon saturated in the SB−C18 material is 5.9 atm at room temperature. After considering the increased solvation of xenon and the lowered temperature, the boiling point at −70 °C for this sample is reasonable. Besides the liquid phase signal, a slight gas phase signal also appears in the spectrum indicating two xenon phases were at equilibrium at this temperature. Another phenomenon in this spectrum is that only the narrower line shape for xenon solvated in the stationary phase was observed, but the broader ones were not observed. The reason could be that the rearrangement of the rigid alkyl chains pushed the xenon atoms out of the immobile area or that the chemical shift anisotropy could be too large to be detected if any xenon atoms were still squeezed between the close chains. The chemical shift of the liquid xenon increased from 227.4 ppm at −70 °C to 257.5 ppm at −110 °C. Owing to the increased liquid phase ^{129}Xe signal, the relative intensity of xenon solvated in the stationary phase became smaller with decreasing temperature, and it is too small to be seen at −100 °C.

At −105 °C, a new peak at 297.4 ppm emerged. Solid xenon has a chemical shift range from 270 to 330 ppm,[9] and xenon has a normal freezing point at −111.7 °C. Thus, this signal should come from solid xenon. This peak was tentatively assigned to solid xenon outside the column material, which could be on top of the column material in the NMR tube. The reason for this assignment is, as will be discussed below, that this xenon could not exchange with the xenon inside the pores and the xenon in the spaces between the particles. As will also be seen shortly, solid xenon inside the pores and between the particles would evolve from the liquid xenon in these spaces. The intensity of the solid xenon signal increased slightly with decreasing temperature. Whereas, its chemical shift increased slightly and reached 306.0 ppm at −150 °C.

When lowering the temperature from −105 to −118 °C, the line shape of the liquid xenon became broader, and from −118 to −150 °C, the single broad signal split into two peaks, which became sharper when the temperature was lowered. The chemical shift of one of the sharper peaks is 279.3 ppm, and the other is 300.3 ppm at −150 °C. This phenomenon can be understood from the point of view of dynamic NMR. At higher temperature (above −105 °C), the xenon atoms exchanged rapidly between the pores and the spaces between the particles. Therefore, only one averaged sharp peak could be observed. When the temperature was lowered, the xenon exchange became slower. Therefore, coalescence appeared at temperatures between −114 and −118 °C. When the temperature was lowered further, the slowed exchange process allowed the two peaks from the xenon in the pores and in the spaces between the particles to be resolved. Thus, we have seen the complete separation of the two peaks below −130 °C. Besides the dynamic NMR process, the chemical shifts of these two peaks also increased during lowering the temperatures. We tentatively assign the peak with smaller chemical shift to the xenon atoms inside the pores, and the other one to xenon atoms in the spaces between the particles. The reason is based on the observation that solid xenon outside the column material has the largest chemical shift, and xenon solvated in the stationary phase has the smallest chemical shift as shown, for example, by the broad peak at 222.3 ppm in the spectrum at −150 °C. This means that xenon atoms interacting more frequently with the surface of the stationary phase showed smaller chemical shifts than those with less probability to do so. A previous study showed that from −110 to −155 °C solid xenon experiences atomic diffusion.[9] At a temperature of −155 °C, the solid xenon underwent a secondary phase transition. When the temperature is below the point of the secondary phase transition, a rigid xenon lattice can exist.[39] This observation supports the explanation of xenon's dynamics shown in Figure 6 between the temperatures of −110 and −150 °C.

As the temperature was lowered, the liquid-phase xenon was transformed to solid at about −110 °C. Further decreasing the temperature slowed xenon diffusion between the pores and the spaces between the silica particles, which in turn broadened the ^{129}Xe line widths. Because of line broadening and the separation of the overlapped chemical shifts, the relative intensity of ^{129}Xe solvated in the stationary phase appeared again below −118 °C. This peak appears as the right shoulder at −118 °C. The chemical shift of this xenon became smaller with decreasing temperature, from 255.0 ppm at −118 °C to 222.3 ppm at −150 °C. A ^{129}Xe NMR study for xenon in a low-density polyethylene showed that xenon was solvated in the amorphous region of the polymer.[40] Similarly, we think that xenon atoms in the stationary phase of the column materials at −150 °C could be likely solvated in the mobile area of the stationary phase. The VT ^{1}H NMR spectra in Figure 4 and the VT ^{129}Xe NMR spectra in Figure 6 provide the complementary information regarding the alkyl chain dynamics and the xenon solvation.

The ^{129}Xe NMR spectra in Figure 6 show the dynamic process of xenon atoms inside the SB−C18 column material at different temperatures. When the spectral resolution allows different peaks to be distinguished and the temperature range is large enough so that the coalescence of the exchanged peaks can be observed, a VT dependent experiment is sufficient to show the xenon diffusion process. However, when the exchange rate is too slow such that the coalescence cannot be obtained, the 2D ^{129}Xe exchange experiment can be used to observe the xenon diffusion process. The spectrum at −70 °C in Figure 6 shows the fast liquid xenon diffusion between the pores and the spaces between the particles of the column material, which is concluded from the single liquid xenon peak. This figure also shows the slow xenon diffusion between the stationary phase and the pores or the spaces between the particles, indicated by partially overlapped but clearly defined two peaks. To observe the slow xenon diffusion, the EXSY experiment was carried out at this temperature. Figure 7 shows the 2D spectrum with a mixing time of 1 ms, where the F_2 projection is shown on top of the 2D spectrum. The wide spread of the off diagonal areas shows that xenon atoms have diffused significantly within the stationary phase and between the stationary phase and the pores or the spaces between the particles within this 1 ms period. The wide spread of the off diagonal area not only reflects xenon's diffusion from one site to another within the stationary phase but also reflects the alkyl chain's dynamics. The motion of the alkyl chains changed the local environment of a xenon atom from one to another during the exchange time. We believe the 2D spectrum shows both the xenon diffusion within the stationary phase and the motion of the alkyl chains of the stationary phase. The mobility of the chains of the mobile area has been directly observed from the VT ^{1}H NMR spectra as shown in Figure 4.

Figure 8 shows the 2D EXSY ^{129}Xe NMR spectrum of the sample at −130 °C. The cross-peaks from the xenon atoms inside the pores and those in the spaces between the particles indicate that the diffusion rate of the solid xenon atoms between these sites was high enough to be observed within 1 ms. At this temperature, the solid xenon peak outside the column

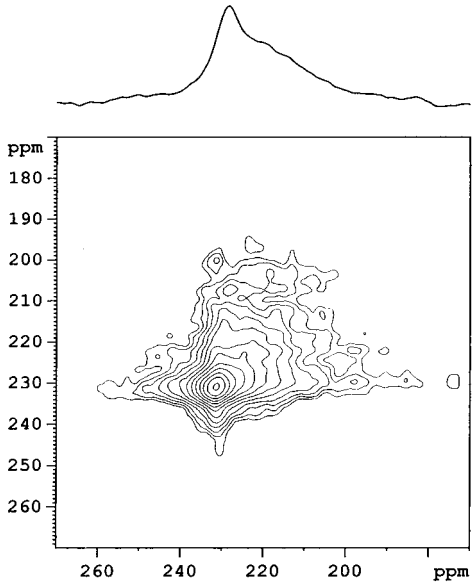

Figure 7. 2D EXSY ^{129}Xe NMR spectrum of the xenon in the SB−C18 column material at −70 °C, where the exchange time of 1 ms was used. The wide spread of the off diagonal areas shows the diffusion of xenon atoms within the stationary phase and the dynamics of the alkyl chains of the stationary phase. The cross-area between the liquid-phase xenon and the xenon solvated in the stationary phase shows the xenon diffusion between the stationary phase and the pores and spaces between the particles.

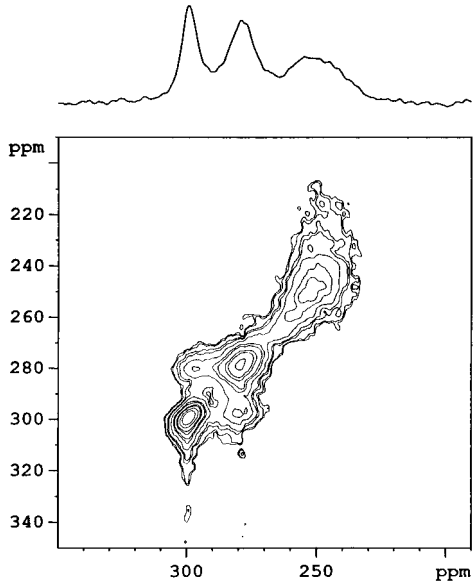

Figure 8. 2D EXSY ^{129}Xe NMR spectrum of the xenon in the SB−C18 column material at −130 °C, where the exchange time of 1 ms was used. The cross-peaks show the xenon diffusion between the xenon atoms possibly inside the pores and in the spaces between the particles.

material is overlapped with the solid xenon peak from the spaces between the particles. It will be shown below that no diffusion between this solid xenon and the other kinds of xenon atoms could be observed. The lack of the off diagonal peaks between the xenon solvated in the stationary phase and that in the pores and the spaces between the silica particles indicates that xenon atoms have been trapped inside the alkyl chains of the stationary phase at this temperature. The lack of obvious spread of the off diagonal area of the xenon signal from the stationary phase indicates that the chain motion was slow enough at this temperature so that not much change of a xenon's local environment was observed within 1 ms.

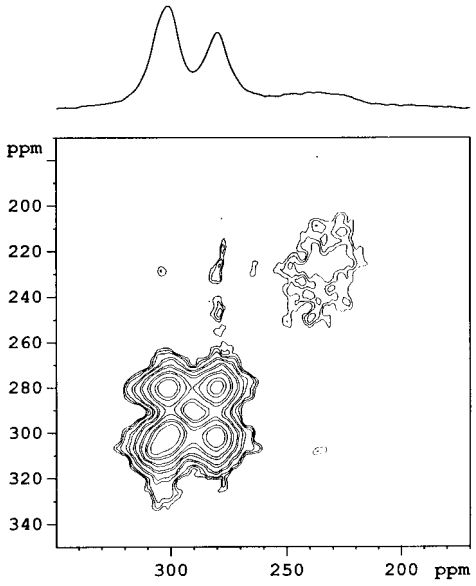

Figure 9. 2D EXSY ^{129}Xe NMR spectrum of the xenon in the SB−C18 column material at −140 °C, where the exchange time of 500 ms was used. The cross-peaks show the xenon diffusion between possibly the pores and the spaces between the silica particles. The wide spread of the off-diagonal area of the ^{129}Xe signal in the stationary phase reflects the slow motion of the alkyl chains in the mobile areas of the stationary phase at this temperature.

The 2D EXSY experiment with 1 ms mixing time was also done at −140 °C. At this temperature, no cross-peaks were observed showing a decreased xenon diffusion rate and chain dynamics. When a mixing time of 500 ms was applied, as shown in Figure 9, cross-peaks were observed between the peaks of xenon from the pores and the spaces between the silica particles, indicating that xenon was not completely frozen even at this temperature. The solid ^{129}Xe signal outside the column material is shown as a prolonged narrow area at the left-lower area of the ^{129}Xe peak from the spaces between the silica particles. The absence of the cross-peaks between this peak and the others means that this xenon did not show any exchange with the xenon inside the pores and the spaces between the particles within 500 ms showing spatially separated areas. As mentioned above, this is one piece of evidence for the assignment of this xenon peak. The appearing lower resolution in this spectrum compared with the spectrum in Figure 6 is due to the applied line broadening to enhance the sensitivity for the 2D NMR spectrum. The spread of the off diagonal area for xenon from the stationary phase was clearly observed at this temperature. This shows that the change of the xenon's local environments in the stationary phase can be observed within 500 ms even at this low temperature. We think that the change of the xenon's local environment could be caused by the slow motion of the alkyl chains in the mobile area of the stationary phase but not by xenon's diffusion among the alkyl chains of the stationary phase because of the lack of xenon diffusion between the stationary phase and the voids of the column material.

IV. Conclusion

The CP MAS ^{29}Si, CP MAS ^{13}C, and MAS ^{1}H NMR spectra of the SB−C18 column material showed the basic stationary-phase structure and mobility. The silica surface was coated with the alkyl chains, $-Si(CH_2-CH-(CH_3)_2)_2(CH_2)_{17}CH_3$, which form the stationary phase of the column material. These alkylsilanes bound on the silica surface with significant mobility at room temperature because of the separation of the chains by

the side groups, $-CH_2-CH-(CH_3)_2$. The VT ^1H NMR spectra revealed the inhomogeneous distribution of the alkyl chains on the silica surface. At low temperatures, the immobile area was formed on the silica surface where the density of the alkyl chains could be higher, and the amorphous area was from the region where the density of the alkyl chains could be lower.

The VT ^{129}Xe NMR spectra and the 2D EXSY ^{129}Xe NMR spectra showed the populations of xenon atoms inside the column material, the interactions of xenon atoms with the stationary phase, the xenon diffusion among the pores, the spaces between the particles and the chains of the stationary phase, and the dynamics of the alkyl chains. Four kinds of xenon were observed in the column material: xenon solvated in the stationary phase, xenon in the pores of the silica particles, xenon in the spaces between the particles of the column material, and xenon outside the materials. Xenon diffusion among the stationary phase, the pores, and the spaces between the silica particles was quite rapid at relatively high temperatures. Even at very low temperatures, xenon could diffuse between the pores and the spaces between the silica particles. However, xenon atoms in the stationary phase were trapped in the amorphous area of the stationary phase at low temperatures. The EXSY^{129}-Xe NMR spectra also showed that the alkyl chains of the mobile area in the stationary phase experienced slow motions even at very low temperatures.

In this paper, we have presented the basic structure, dynamics, and interaction of the SB−C18 column material and the mobile phase xenon atoms. This research demonstrated that the solid-state NMR and the mobile phase ^{129}Xe NMR provide complementary information for the study of column materials.

Acknowledgment. Richard Perrigan is thanked for his technical assistance in the NMR experiments.

References and Notes

(1) Scott, R. P. W. *Techniques and Practice of Chromatography*; Marcel Dekker: New York, 1995.
(2) Rohards, K.; Haddad, P. R.; Jackson, P. E. *Principle and Practice of Modern Chromatogrphic Methods*; Academic Press: New York, 1994.
(3) Smith, R. M. *Gas and Liquid Chromatography in Analytical Chemistry*; Wiley: New York, 1988.
(4) Pursch, M.; Vanderhart, D. L.; Sander, L. C.; Gu, X.; Nguyen, T.; Wise, S. A.; Gajewski, D. A. *J. A. Chem. Soc.* **2000**, *122*, 6997.
(5) Pursch, M.; Sander, L. C.; Egelhaaf, H.-J.; Raitza, M.; Wise, S. A.; Oelkrug, D.; Albert, L. *J. A. Chem. Soc.* **1999**, *121*, 3201.
(6) Pursch, M.; Strohschein, S.; Haendel, H.; Albert, K. *Anal. Chem.* **1996**, *68*, 386.
(7) Pursch, M.; Jaeger, A.; Schneller, T.; Brindle, R.; Albert, K.; Lindner, E. *Chem. Mater.* **1996**, *8*, 1245.
(8) Pursch, M.; Sander, L. C.; Albert, K. *Anal. Chem.* **1996**, *68*, 4107.
(9) Raftery, D.; Chmelka, B. F. *NMR basic principle Progress* **1994**, *30*, 111.
(10) Ito, T.; Fraissard, J. *J. Chem. Phys.* **1982**, *76*, 5225.
(11) Ripmeester, J. A. *J. Am. Chem. Soc.* **1982**, *104*, 289.
(12) Fraissard, J., Zeitsch. *Phys. Chem.* **1987**, *152*, 159.
(13) Dybowski, C.; Bansal, N.; Duncan, T. M. *Ann. Rev. Phys. Chem.* **1991**, *42*, 433.
(14) Chmelka, B. F.; Raftery, D.; McCormick, A. V.; L. Menorval, C.d.; Levine, R. D.; Pines, A. *Phys. Rev. Lett.* **1991**, *66*, 580.
(15) Larsen, R. G.; Shore, J.; Schmidt-Rohr, K.; Emsley, L.; Long, H.; Pines, A.; Janicke, M.; Chmelka, B. F. *Chem. Phys. Lett.* **1993**, *214*, 220.
(16) Springuel-Huet, M.-A.; Nosov, A.; Karger, J.; Fraissard, J. *J. Phys. Chem. B* **1996**, *100*, 7200.
(17) Moudrakovski, I. L.; Ratcliffe, C. I.; Ripmeester, J. A. *J. Am. Chem. Soc.* **1998**, *120*, 3123.
(18) Pietrass, T.; Kneller, J. M.; Assink, R. A.; Anderson, M. T. *J. Phys. Chem. B* **1999**, *103*, 8837.
(19) Laboriau, A.; Panjabi, G.; Enderle, B.; Pietrass, T.; Gates, B. C.; Earl, W. L.; Ott, K. C. *J. Am. Chem. Soc.* **1999**, *121*, 7674.
(20) Kentgens, A. P. M.; Boxtel, H. A. v.; Verweel, R. J.; Veeman, W. S.; *Macromolecules* **1991**, *24*, 3712.
(21) Tomaselli, M.; Meier, B. H.; Robyr, P.; Suter, U. W.; Ernst, R. R. *Chem. Phys. Let.* **1993**, *205*, 145.
(22) Schantz, S.; Veeman, W. S. *J. Polym. Sci. Part B: Polym. Phys.* **1997**, *35*, 2681.
(23) Koons, J. M.; Wen, W.-Y.; Inglefield, P. T.; Jones, A. A. *Polym. Mater. Sci. Eng.* **1997**, *76*, 433.
(24) Junker, F.; Veeman, W. S. *Macromolecules* **1998**, *32*, 7010.
(25) Heink, W.; Kaerger, J.; Pfeifer, H.; Stallmach, F. *J. Am. Chem. Soc.* **1990**, *112*, 2175.
(26) Jeener, J.; Meier, B. H.; Bachmann, P.; Ernst, R. R. *J. Chem. Phys.* **1979**, *71*, 4546.
(27) Perrin, C. L.; Dwyer, T. J. **1990**, *90*, 935.
(28) Macura, S.; Westler, W. M.; Markley, J. C. *Methods Enzymol.* **1994**, *239*, 106.
(29) Veeman, W. S.; Maas, W. E. J. R. *NMR Basic Principle and Progress* **1994**, *32*, 129.
(30) Engelhardt, G.; Koller, H. *Solid State NMR* **1993**, *31*, 1.
(31) Clauss, J.; Schmidt-Rohr, K.; Adam, A.; Boeffel, C.; Spiess, H. *Macromolecules* **1992**, *25*, 5208.
(32) Pawsey, S.; Yach, K.; Halla, J.; Reven, L. *Langmuir* **2000**, *16*, 3294.
(33) Maciel, G. E.; Ellis, P. D. In *NMR techniques in Catalysis*; Bell, A. T., Pines, A., Eds.; Marcel Dekker: New York, 1994; p 231.
(34) Maciel, G. E.; Bronnimann, C. E.; Zeigler, R. C.; Chuang, I.-S.; Kinney, D. R.; Keiter, E. A. In *The Colloid Chemistry of Silica*; Bergna, H. E., Ed.; Adv. Chem. Ser. 234; American Chemical Society: Washington, DC., 1994; p 269.
(35) Kinney, D. R.; Chuang, I.-S.; Maciel, G. E. *J. Am. Chem. Soc.* **1993**, *115*, 6786.
(36) Doremierux-Morin, C.; Heeribout, L.; Dumousseaux, C.; Fraissard, J.; Hommel, H.; Legrand, A. P. *J. Am. Chem. Soc.* **1996**, *118*, 13040.
(37) Ba, Y.; Ripmeester, J. A. Multiple quantum filtering and spin exchange in solid-state nuclear magnetic resonance. *J. Chem. Phys.* **1998**, *108*(20), 8589−14.
(38) Ba, Y. Ph.D. Thesis, Gerhard-Mercarter University, Duisburg: Duisburg, 1995.
(39) Yen, W. M.; Norberg, R. E. *Phys. Rev.* **1963**, *131*, 269.
(40) Stengle, T. R.; Williamson, K. L. *Macromolecules* **1987**, *20*, 1428.